Co^{II} Complexes with Mixed Amino-*N* and Thiolato-*S* Donor Sets − Structural Characterization and Electronic Properties of a Stable Bis(μ-thiolato)-Bridged Binuclear Co^{II} Complex

Didier Bonnet,[a] Philippe Leduc,[a] Eckhard Bill,[b] Geneviève Chottard,[c] Daniel Mansuy,[a] and Isabelle Artaud*[a]

Keywords: Cobalt / S ligands / Electrochemistry / Raman spectroscopy / N ligands

Two different ligands [$S_2N_3^{py}$] and [S_2N_2], prepared from 2,6-bis[1-(2-mercaptoanilino)ethyl]pyridine and 2,3-bis(2-mercaptoanilino)butane, respectively, have been used to investigate cobalt coordination with mixed amine nitrogen/sulfur donor sets. The pentadentate [$S_2N_3^{py}$] ligand gave rise to a mononuclear [$Co^{II}(S_2N_3^{py})$] complex, which was found to be stable only at low temperatures under argon, and was characterized as having a high-spin Co^{II} state on the basis of ^1H NMR and EPR measurements. In contrast, the tetradentate [S_2N_2] ligand led to a binuclear bis(μ-thiolato) $[Co^{II}(S_2N_2)]_2$ complex, the structure of which was solved by X-ray crystallography. Each Co^{II} centre was found to reside in an N_2S_3 square-pyramidal environment in the crystal, the two Co atoms being bridged by one of the two thiolates of an [S_2N_2] ligand. On the basis of the temperature dependence of the magnetic susceptibility, the two Co^{II} centres were found to be in a low-spin state and slightly antiferromagnetically coupled with an absolute J value of less than 3 cm^{-1}. In aerated CH_2Cl_2 in the presence of CH_3SO_3H, the binuclear complex proved to be stable in its mixed valence state, [Co^{II}/Co^{III}], which could be converted back to [Co^{II}/Co^{II}] upon addition of NBu_4OH in MeOH. Three different stable oxidation states could be characterized by electro- and spectroelectrochemistry (E [Co^{II}/Co^{II}]/[Co^{II}/Co^{III}] = –0.19 V, E [Co^{II}/Co^{III}]/[Co^{III}/Co^{III}] = 0.2 V vs. SCE). The electronic spectrum of the [Co^{II}/Co^{II}] state features a broad absorption at 630 nm and a sharp band at 565 nm, while that of the [Co^{II}/Co^{III}] state shows two bands at 657 and 800 nm. The Raman spectrum of the [Co^{II}/Co^{II}] state was found to be dominated by a Co_2S_2 core vibration at 223 cm^{-1}, which proved to be strongly resonance-enhanced within the 565 nm absorption band, thus giving a sound basis for its assignment as an S→Co^{II} charge-transfer band. For the [Co^{II}/Co^{III}] state, a significant resonance Raman enhancement was observed within the 657 nm absorption band for a larger number of vibrations involving the Co_2S_2 core as well as the phenyl ring.

Introduction

While mixed nitrogen/sulfur coordination spheres about transition metals are often encountered in the active sites of iron-, copper-, and zinc-containing proteins,[1] only a few enzymes have a cobalt centre with a mixed N/S donor set, such as ATP sulfurylase,[2] nitrile hydratase,[3] and peptide deformylase.[4] The first two of these possess a native cobalt centre, which has been spectroscopically characterized. In contrast, peptide deformylase, which naturally contains iron or nickel as the metal centre for catalytic amide hydrolysis, has been characterized by X-ray crystallography of a cobalt-substituted form. ATP sulfurylase and peptide deformylase contain four-coordinate Co^{II} centres, with NS_3 and N_2SO donor sets, respectively. Co nitrile hydratases have a low-spin Co^{III}, which is thought to be six-coordinate with an N_2S_3 core, by analogy with the more extensively characterized iron-containing enzymes. These newly identified cobalt biological systems have fostered a growing interest in the investigation of new cobalt complexes with mixed nitrogen/sulfur coordination spheres.

In this study, we describe the synthesis and the spectroscopic characterization of two new Co^{II} complexes, a [$Co^{II}(S_2N_3^{py})$] mononuclear species and a $[Co^{II}(S_2N_2)]_2$ dimer derived from 2,6-bis[1-(2-mercaptoanilino)ethyl]pyridine and 2,3-bis(2-mercaptoanilino)butane, respectively. The binuclear complex, for which the structure has been solved, is easily converted in CH_2Cl_2 into the mixed valence state [Co^{II}/Co^{III}] and into the fully oxidized state [Co^{III}/Co^{III}].

Results and Discussion

Synthesis of the Ligands and Complexes

Thiolate-ligated zinc template complexes [S_2N_2Zn] (**1**) and [$S_2N_3^{py}Zn$] (**3**) (Scheme 1) were prepared in three steps according to published procedures:[5−7] (i) condensation of 2-aminobenzenethiol with 2,3-butanedione and 2,6-diacetylpyridine for **1** and **3**, respectively, (ii) opening of the resulting bis(benzothiazolyl) compound with zinc acetate, and (iii) reduction[6] of the zinc complex imine functions with $NaBH_4$.

[a] Laboratoire de Chimie et Biochimie Pharmacologiques et Toxicologiques, CNRS UMR 8601,
45 rue des Saints-Pères, 75270 Paris Cedex 06, France
Fax: (internat.) + 33-1/42868387
E-mail: artaud@biomedicale.univ-paris5.fr
[b] Max-Planck-Institut für Strahlenchemie,
Stiftstrasse 34−36, 45470 Mülheim an der Ruhr, Germany
[c] Laboratoire de Chimie Inorganique et Matériaux Moléculaires, CNRS ESA 7071, Université Pierre et Marie Curie,
75252 Paris Cedex 05, France

Supporting information for this article is available on the WWW under http://www.wiley-vch.de/home/eurjic or from the author.

  1434−1948/01/0606−1449 $ 17.50+.50/0

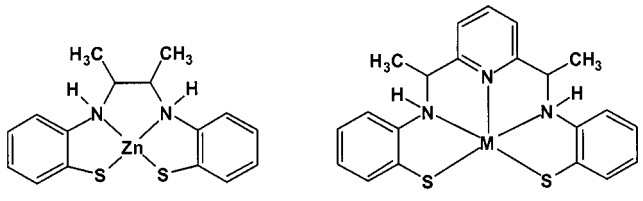

Scheme 1

After demetallation of the zinc derivatives under basic conditions, the free dithiolate ligands were metallated with $CoCl_2 \cdot 6H_2O$ in the presence of a slight excess of base. Complex $[Co^{II}(S_2N_2)]_2$ (**2**) was isolated as a microcrystalline purple powder by precipitation from a solution in dichloromethane by the addition of pentane. In contrast to complex **2**, which was found to be air-stable, complex $[Co^{II}(S_2N_3{}^{py})]$ (**4**), isolated from DMF by precipitation with diethyl ether, proved to be sensitive to trace amounts of dioxygen and consequently had to be handled under argon and at low temperature.

Characterization of Complex 2

Crystal Structure

Single crystals of **2** were grown by vapor diffusion of pentane into a dichloromethane solution of the complex. The ORTEP diagram of the neutral complex **2** is shown in Figure 1. Collection parameters and selected interatomic distances along with bond angles are listed in Table 1 and 2, respectively.

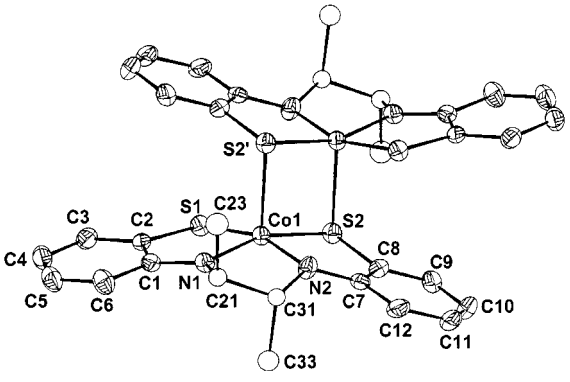

Figure 1. Thermal ellipsoid plot (50% probability level) of the neutral complex $[L_1Co^{II}]_2$ (**2**); carbon atoms C21, C23, C31, C33 are disordered and correspond to two equiprobable *trans* conformations of the methyl groups

The X-ray structure of the binuclear complex **2** reveals a nearly ideal square-pyramidal environment for each cobalt centre, with the four atoms (2 N and 2 S) of an S_2N_2 ligand in the mean equatorial plane and the thiolate of the second $[S_2N_2Co]$ moiety in the axial position. The two cobalt centres are connected through an inversion centre. The average lengths of the Co−S and Co−N bonds in the mean plane are 2.17 Å and 1.85 Å, respectively. These values are in agreement with those previously reported for a binuclear Co^{II} complex derived from thiosalen $[tsalenCo^{II}]_2$.[8] The four atoms (2 N and 2 S) are almost coplanar and deviate by no more than 0.07 Å from the mean plane, while the cobalt cation is displaced by 0.32 Å towards the axial ligand. With a dihedral angle between the (C1−C6, S1, N1) and (C7−C12, S2, N2) planes of only 4°, the two aromatic rings and the S_2N_2 core of the ligand are almost coplanar. The axial Co−S distance (2.37 Å) of the μ-thiolato bridge is 0.2 Å longer than the Co−S bond in the mean plane and is similar to that observed in $[tsalenCo^{II}]_2$ [Co−S(bridging) 2.44 Å].[8] Such a sulfur-bridging bis(μ-thiolato) mode has previously been observed in binuclear Co^{II} [8] and Fe^{II} [9] complexes derived from a tetradentate tsalen (N_2S_2) ligand, as well as in binuclear Co^{III} complexes derived from a

Table 1. Crystallographic data for $[S_2N_2Co^{II}]_2$ (**2**)

Emprical formula	$C_{32}H_{36}N_4S_4Co_2$
Molecular mass	722.8
a [Å]	11.698(4)
b [Å]	8.993(3)
c [Å]	15.064(5)
β [°]	92.38(3)
V [Å^3]	1583.3(9)
Z	2
Crystal system	monoclinic
Space group	$P2_1/n$
μ [cm^{-1}]	13.3
ρ [g·cm^{-3}]	1.52
Diffractometer	CAD4 Enraf−Nonius
T [K]	295
No. of data collected	3132
No. of unique data collected	2782 (R_{int} = 0.06)
No. of unique data used for refinement	1712 $(F_o)^2 > 3\sigma(F_o)^2$
Radiation	Mo-K_α (λ = 0.71069 Å)
$R = \Sigma\|\|F_o\| - \|F_c\|\|/\Sigma\|F_o\|$	0.0529
$Rw = [\Sigma w(\|F_o\| - \|F_c\|)^2/\Sigma w\|F_o\|^2]^{1/2}$	0.0630

Table 2. Selected bond lengths [Å] and angles [°] in **2**

Co(1)−Co(1′)	3.038(1)	Co(1)−S(1)	2.161(2)
Co(1)−S(2)	2.185(2)	Co(1)−S(2′)	2.372(2)
Co(1)−N(1)	1.840(5)	Co(1)−N(2)	1.852(5)
S(1)−C(2)	1.712(6)	S(2)−C(8)	1.739(6)
N(1)−C(1)	1.349(8)	N(1)−C(21)	1.47(2)
N(1)−C(22)	1.49(1)	N(2)−C(7)	1.350(8)
N(2)−C(31)	1.54(1)	N(2)−C(32)	1.46(1)
C(1)−C(2)	1.428(9)	C(7)−C(8)	1.424(9)
C(21)−C(31)	1.50(2)	C(22)−C(32)	1.59(2)
S(1)−Co(1)−S(2)	94.33(7)	S(1)−Co(1)−S(2′)	96.43(6)
S(2)−Co(1)−S(2′)	96.46(6)	S(1)−Co(1)−N(1)	87.8(2)
S(2)−Co(1)−N(1)	160.8(2)	S(2)−Co(1)−N(1)	102.3(2)
S(1)−Co(1)−N(2)	161.5(2)	S(2)−Co(1)−N(2)	87.8(2)
S(2)−Co(1)−N(2)	101.6(2)	N(1)−Co(1)−N(2)	84.3(2)
Co(1)−S(1)−C(2)	98.1(2)	Co(1)−S(2)−Co(1)	83.54(6)
Co(1)−S(2)−C(8)	97.6(2)	Co(1)−S(2′)−C(8′)	107.2(2)
Co(1)−N(1)−C(1)	121.8(4)	Co(1)−N(1)−C(21)	118.7(6)
Co(1)−N(1)−C(22)	113.8(6)	Co(1)−N(2)−C(7)	121.9(4)
Co(1)−N(2)−C(31)	114.3(6)	Co(1)−N(2)−C(32)	116.4(6)

pentadentate N_3S_2 ligand[10] or a bidentate S_2 ligand.[11,12] As for all the other Co(μ-SR)$_2$Co dimers, the two sulfur atoms of the bridge and the two Co atoms are almost planar with a slight tetrahedral distortion, the (Co1−S2−Co′1) angle being close to 90° (97°). The structural parameters of **2** confirm the presence of two amine ligands with C21−N1 and C31−N2 bond lengths of 1.47 Å and 1.54 Å, respectively. If a dehydrogenation had occurred, the C−N distances of the corresponding imines would have been in the range of 1.2−1.3 Å.[13,14] Interestingly, the ESI^+ mass spectrum of **2** displays a 100% peak at $m/z = 718$, which corresponds to the mass of the dimer after the loss of four protons. This could result from the formation of one imine moiety per monomer during the ionization process. Such a dehydrogenation reaction of $[S_2N_2]$ has previously been observed in the one-electron reduction of a dioxomolybdenum complex $[S_2N_2Mo^{VI}O_2]$.[15]

Magnetism, EPR, and ^{1}H NMR

The temperature dependence of the magnetic susceptibility of a solid sample of the binuclear complex **2** was recorded over the range 290−4 K. The effective magnetic moment was found to have a value of 2.92 μB (1.46 μB per Co) at 290 K and dropped to 1.4 μB at 4 K (Supporting Information). This behaviour is consistent with the presence of two low-spin Co^{II} ions, antiferromagnetically coupled with an absolute J value of less than 3 cm^{-1} [$H = -2J\cdot\boldsymbol{S}_1\cdot\boldsymbol{S}_2$] (a tentative fit leading to $J = -\mathbf{1.6}$ cm^{-1} is shown in the Supporting Information). As expected for two antiferromagnetically coupled Co^{II} ions, complex **2** is EPR-silent. However, its ^{1}H NMR spectrum in [D$_6$]DMSO (Supporting Information) at 290 K extends over 270 ppm and is consistent with the two Co^{II} centres being only slightly coupled at this temperature. The ^{1}H NMR spectrum is completely symmetrical featuring only six shifted resonances. This suggests that the interconversion between the two conformations observed in the solid state is rapid in relation to the NMR time scale. Moreover, the S_2N_2 ligand seems to be planar with such a weak interaction between the two cobalt centres that the complex could be regarded as a monomer. The proton resonances of the ligand were assigned on the basis of their chemical shifts, relative integrals, and ^{1}H longitudinal relaxation times (T_1) correlated to the Co···H distances available from the crystal structure, as described in the Exp. Sect. The signals at δ = −18 (12 H) and δ = +166 (4 H) were assigned to the methyl protons and to the equivalent H(21) protons, respectively. The four aromatic rings are equivalent. However, it is difficult to assign the resonances to H(3) and H(6) as well as to H(4) and H(5). The protons H(4) and H(5), being furthest from the cobalt centre, have the largest T_1 values and are believed to be responsible for the signals at δ = +12 and/or δ = +16.5. Finally, the resonances at δ = −107 and δ = −111 were assigned to H(3) and/or H(6).

Electronic Spectra and Stability Towards O_2

In DMF under anaerobic or aerobic conditions, the electronic spectrum of complex **2** exhibits a complex pattern, as is often reported for Co^{II} complexes. It consists of a broad band centred at 630 nm [1000 L mol^{-1} cm^{-1}] with secondary maxima on the high energy side that are roughly spaced by 1300 cm^{-1}, the first maximum appearing at 565 nm [2500 L mol^{-1} cm^{-1}]. The 565-nm band is assigned to a thiolate-to-cobalt S→Co^{II} charge-transfer band on the basis of the resonance Raman experiments described below, whereas the broad band located at 630 nm should correspond to the superimposition of several d-d transitions very close in energy. In CH_2Cl_2 under anaerobic conditions, complex **2** not only exhibits an absorption at 565 nm, as it does in DMF, but also two other bands at 657 nm and 800 nm. Upon exposure to air, the blue-purple CH_2Cl_2 solution turned deep-blue and the spectrum obtained thereafter featured only a sharp absorption at 657 nm (5500 L mol^{-1} cm^{-1}) and a small one at 800 nm (1400 L mol^{-1} cm^{-1}). Thus, the spectrum of the dimer in CH_2Cl_2 under argon is that of a mixture of two species **2** and **2a** characterized by absorptions at 565 nm and 657/800 nm, respectively. In this solvent, complex **2** is obtained exclusively after adding 1 equiv. of NBu_4OH in MeOH, while complex **2a** is formed after adding 1 equiv. of CH_3SO_3H in the presence of dioxygen. The absolute requirement of dioxygen to convert **2** into **2a** under acidic conditions suggests that **2a** is probably an oxidized state of **2**. Finally, we note that under the conditions defined above, the conversion of **2** into **2a** is reversible, both in DMF and in CH_2Cl_2 [Equation (1)].

$$\mathbf{2} \underset{NBu_4OH,\ MeOH}{\overset{MeSO_3H,\ air}{\rightleftharpoons}} \mathbf{2a} \qquad (1)$$

Electro- and Spectroelectrochemistry

The cyclic voltammogram of **2** in DMF at 25 °C displays two quasi-reversible waves of equal intensity located at $E_1 = -0.19$ and $E_2 = +0.05$ V vs. SCE (Supporting Information). This indicates that **2** retains its binuclear [Co^{II}−Co^{II}] structure in DMF solution. On using NBu_4PF_6 instead of NBu_4Cl as the supporting electrolyte, the second oxidation wave was seen to be shifted from +0.05 to +0.2 V and became irreversible, suggesting that chloride anions were required to observe a reversible second oxidation of **2**.

The cyclic voltammogram of **2** obtained at 25 °C in CH_2Cl_2 containing NEt_4Cl as the supporting electrolyte exhibits two quasi-reversible waves as in DMF, located at $E_1 = -0.19$ V and $E_2 = +0.2$ V (Figure 2, A). Nevertheless, in contrast to DMF solution, the zero-current potential in CH_2Cl_2 ($E_0 = -0.19$ V) corresponds to the first potential E_1, indicating that, in agreement with the UV/Vis experiments, both [$Co^{II}Co^{II}$] (**2**) and its first oxidized species [$Co^{II}Co^{III}$]$^+$ (**2a**) are present in solution. As expected for a metal-centred oxidation, the shapes of the cyclic voltammograms of the pure species **2a** and **2**, recorded after the addition of 1 equiv. of $MeSO_3H$ in the presence of dioxygen or of 1 equiv. of NBu_4OH, respectively, remained identical. Only the zero-current potentials were shifted, from $E_0' =$

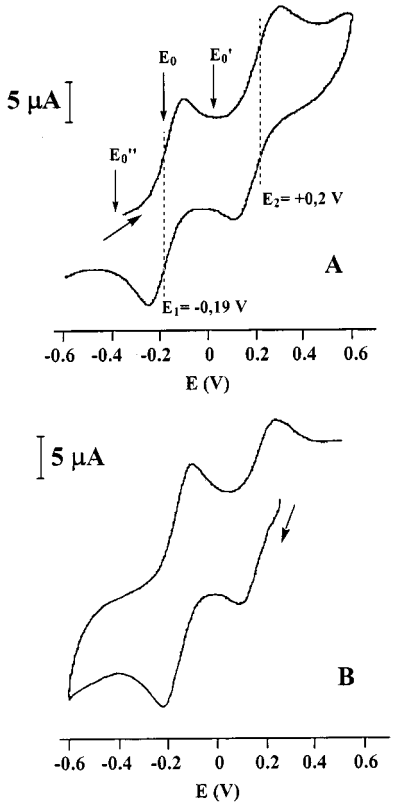

Figure 2. Cyclic voltammograms in CH_2Cl_2 solution at 25 °C (0.1 M Bu_4NCl; glassy carbon working electrode and saturated calomel reference electrode; 50 mV s^{-1}): A: $[Co^{II}Co^{II}]$ compound **2** ($\approx 10^{-3}$ M) obtained after addition of 1 equiv. of Bu_4NOH to a solution of $[S_2N_2Co]_2$ in dichloromethane; E_1 and E_2 correspond to $E_{1/2}$ potentials, E_0, E_0', and E_0'' to the zero-current potentials observed for the initial **2**/**2a** mixture in CH_2Cl_2 and for the unique species **2a** and **2** (obtained after addition of $MeSO_3H$ or Bu_4NOH), respectively; B: **2b** produced by electrolysis of a solution of **2a** at +0.45 V

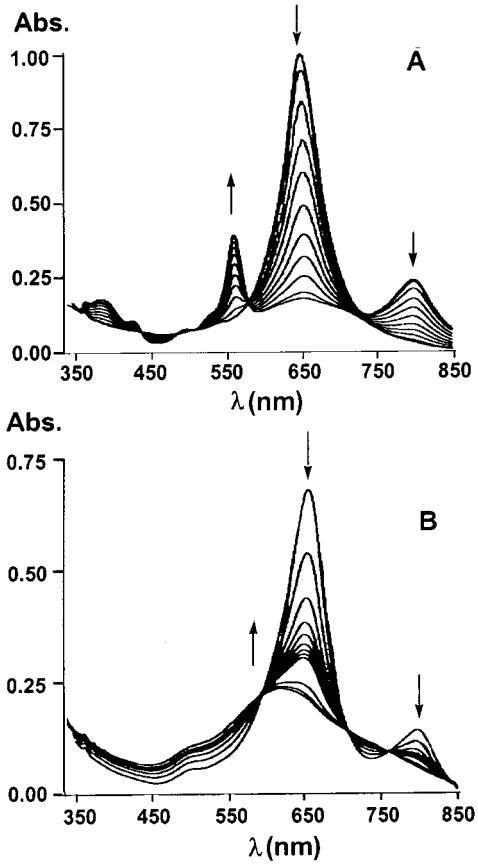

Figure 3. Spectroelectrochemistry of **2a** in CH_2Cl_2 at 25 °C: one-electron reduction (A) (isosbestic points: 435, 490, 585, 730 nm) and one-electron oxidation (B) (isosbestic points: 595, 715, and 795 nm) (conditions: [**2a**] $\approx 10^{-3}$ M with 0.1 M Bu_4NCl); the final spectra correspond to those of **2** and **2b**, respectively

−0.05 V for **2a** to $E_0'' = -0.27$ V for **2** (Figure 2, A). Any ligand-centred oxidation can be excluded since, using the zinc derivative **1**, the ligand is irreversibly oxidized in DMF at 560 mV vs. SCE.

To further investigate the electronic properties of the dimer, spectroelectrochemical reduction (Figure 3, A) and spectroelectrochemical oxidation (Figure 3, B) of **2a** were performed in CH_2Cl_2. Indeed, upon one-electron reduction of **2a** at −0.5 V, the characteristic UV/Vis spectrum of **2** was obtained. The one-electron oxidation of **2a** at 0.6 V led to a new species **2b**, exhibiting a broad absorption at 625 nm. Both reduction and oxidation were found to be reversible. The cyclic voltammogram of **2b** (Figure 2, B) displays the same characteristic binuclear pattern as seen for **2** and **2a**, with the exception of a zero-current potential of +0.45 V. Consequently, compound **2b** is proposed to be the fully oxidized binuclear Co^{III} complex $[LCo^{III}]_2^{2+}$. However, as chloride anions greatly increased its stability, it would be better described as a six-coordinate species $[LCo^{III}Cl]_2$.

Hence, complex **2** represents the first reported example of a bis(μ-thiolato) binuclear Co^{II} complex with a mixed nitrogen/sulfur environment, exhibiting three stable reversible oxidation steps in solution. Ghilardi et al.[16] have previously described a sulfide-bridged binuclear Co^{II}/Co^{III} complex and its corresponding di-Co^{II} and di-Co^{III} complexes, which were obtained by $NaBH_4$ reduction and $NOBF_4$ oxidation, respectively. However, none of the reduced or oxidized states were stable in solution. Both $[Co^{II}/Co^{II}]$ and $[Co^{II}/Co^{III}]$ states of the dimer were easily accessible in solution by treatment with acid or base. A similar reduction of Fe^{III} complexes in the presence of HO^- in MeOH or DMSO has been reported.[17] However, all attempts to crystallize the $[Co^{II}/Co^{III}]$ species failed since it reverted back to the $[Co^{II}/Co^{II}]$ complex in the solid state.

Raman Spectroscopy

The resonance Raman spectra of the $[Co^{II}/Co^{II}]$ and $[Co^{II}/Co^{III}]$ complexes in DMF solution, both recorded using an excitation frequency close to their respective visible absorption maxima, are shown in Figure 4. In the spectrum of **2**, two main bands are seen at 223 and 1295 cm^{-1}, while in that of **2a**, besides the same two bands, which are shifted

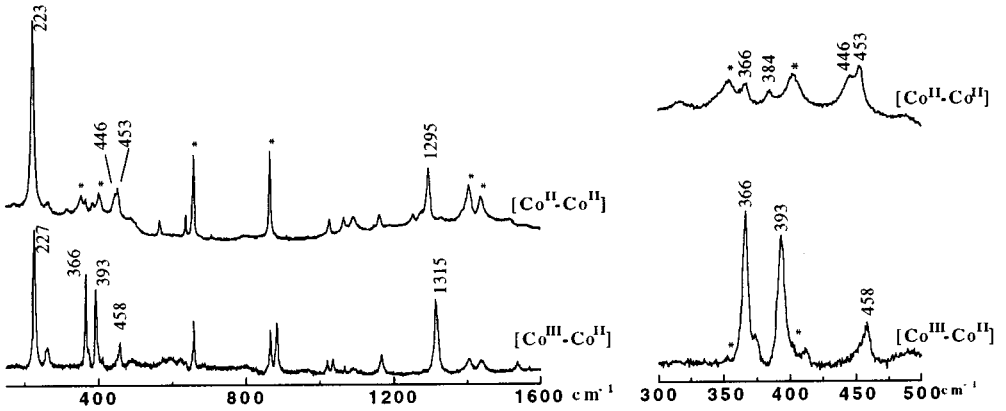

Figure 4. Resonance Raman spectra in DMF solution of the [$Co^{II}Co^{II}$] dimer **2** obtained with 568-nm excitation (upper trace) and of the [$Co^{II}Co^{III}$] complex **2a** obtained with 647-nm excitation (lower trace); * denotes solvent bands

to 227 and 1315 cm^{-1}, three additional bands with comparable intensities are seen at 366, 393, and 1019 cm^{-1}. Weaker bands are seen in the 1000−1150 cm^{-1} region for both complexes and in the 350−650 cm^{-1} region for the [Co^{II}/Co^{II}] complex.

The excitation profiles of these bands were established: They revealed a maximum at a wavelength close to the maximum of the strongest visible absorption band. For the [Co^{II}/Co^{II}] complex (Figure 5, A), an extremely strong enhancement factor was obtained for the 223 cm^{-1} band at 565 nm, at the maximum of the narrow absorption band; the other low-frequency bands were slightly enhanced, as were the high-frequency bands, with the exception of that at 1295 cm^{-1}, which displayed the second highest enhancement factor. We also note the selectivity of the enhancement of the low-frequency bands within the 565 nm band; in contrast, the high-frequency bands show residual intensity on the blue side of the absorption band. This is consistent with the assignment of the latter to phenyl ring vibrations, and of the former to cobalt ligand modes. The very strong and selective enhancement of the 223 cm^{-1} band and the presence of its first harmonic at 446 cm^{-1} suggest an A-term resonance (Franck−Condon mechanism). For the [Co^{II}/Co^{III}] complex (Figure 5, B), the low-frequency bands at 225, 366, and 393 cm^{-1} show the highest enhancement factors, followed by the 458, 1165, and 1315 cm^{-1} bands, the 1019 and 882 cm^{-1} bands being less enhanced.

To the best of our knowledge, no Raman data are available for binuclear bis(μ-thiolato)cobalt complexes, whereas numerous data on Fe−S and Cu−S vibrations have been reported, mainly for Fe−S and Cu−S proteins and some of their model compounds.[18,19] The M−S stretching vibrations have been located in the region 280−430 cm^{-1}. Raman bands in the region 400−280 cm^{-1}, resonance-enhanced within an absorption band at 510 nm, have also been observed for polymeric (thiolato)Co^{III} complexes, the structures of which have not been precisely determined.[20] Therefore, due to its low frequency, the most prominent band of the Co^{II} dimer cannot be assigned to a Co−S stretching vibration; it might correspond to the totally sym-

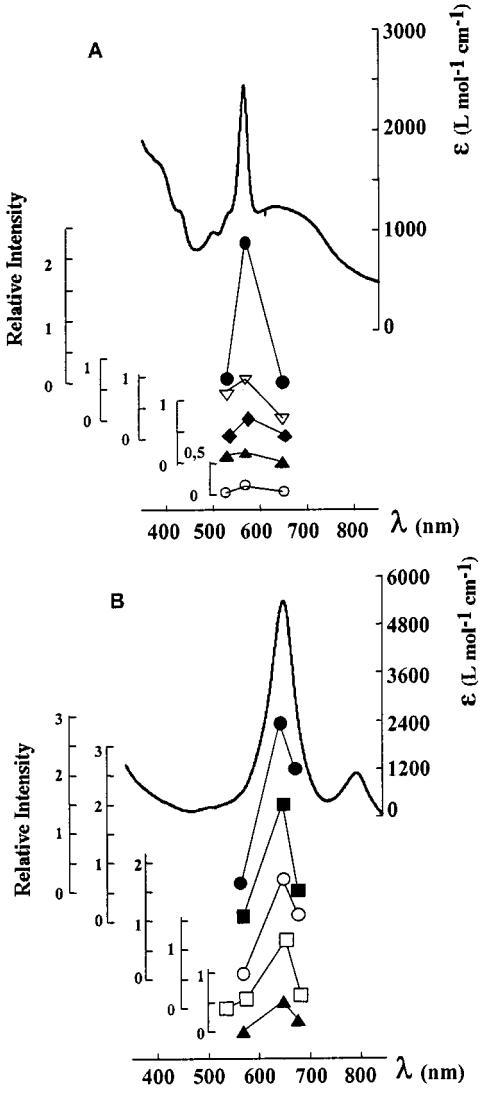

Figure 5. Absorption spectra and excitation profiles of the main Raman bands: A: **2**: ● 222 cm^{-1}, ○384 cm^{-1}, ◆ 453 cm^{-1}, ▲ 1162 cm^{-1}, ▽ 1295 cm^{-1}; B: [$Co^{II}Co^{III}$] dimer **2a**: ● 225 cm^{-1}, ■ 367 cm^{-1}, ▲ 459 cm^{-1}, □ 882 cm^{-1}, ○ 1315 cm^{-1}

metric bending mode of the Co1−S2−Co′1−S′2 core (involving both Co−S−Co and S−Co−S angular deformations): An analogous vibration has been observed at ca. 200 cm^{-1} for the Fe_2S_2 core in the model compound Fe_2S_2(*o*-xylenedithiolate)$_2$ [21] and has been considered as having Fe−Fe stretching character. The two stretching vibrations of the Co_2S_2 core might be located at 453 cm^{-1} (symmetric ring breathing) and 384 cm^{-1}, as these bands show significant enhancement within the 565-nm absorption band. The same three bands are present in the [Co^{II}/Co^{III}]$^+$ complex spectrum at slightly higher frequencies, i.e. 227, 458, and 393 cm^{-1}, respectively. The other strong low-frequency band at 366 cm^{-1} might be the $Co-S_{terminal}$ stretching mode that showed increased intensity in the mixed valence dimer.

Among the high-frequency bands, which correspond to vibrations of the phenylthiolate moiety, the band at ca. 1300 cm^{-1} was seen to be significantly enhanced: It might be analogous to the 1320 cm^{-1} band observed for catecholate complexes of human tyrosine hydroxylase, which has been assigned to a ring deformation of *ortho*-disubstituted benzene and proposed as a marker for bidentate catecholate-type coordination.[22]

Characterization of Complex 4

The electronic spectrum of **4** in DMF features an intense absorption at 420 nm [3000 mol^{-1} L cm^{-1}] and two weak bands at 640 and 350 nm. In the presence of dioxygen, a rapid change in the visible spectrum was observed, associated with complete degradation of the complex. This complex not only proved to be unstable towards dioxygen, but it had to be kept at low temperatures both in solution and in the solid state, otherwise it was very rapidly degraded. For this reason, we were unable to obtain a reliable elemental analysis or crystals suitable for X-ray analysis. Consequently, complex **4** could only be characterized at low temperatures by EPR and ^{1}H NMR spectroscopy. The X-band EPR spectrum in deaerated frozen DMF solution at 10 K (Figure 6) is consistent with a high-spin Co^{II} mononuclear complex. It shows a broad resonance at $g = 4.3$ and a small component at $g = 2$, the second derivative of which exhibits an eight-line hyperfine structure with a spacing of 100 G, a value typical of high-spin Co^{II} complexes. The ^{1}H NMR spectrum of **4** in [D_7]DMF, recorded at −40 °C under argon (Supporting Information), shows the 17 expected sharp signals in the range $\delta = -27$ to +161. The two methyl resonances were assigned to the signals at $\delta = +18$ and +14 on the basis of their integrals, which corresponded to three protons, whereas all the other peaks integrated as one proton.

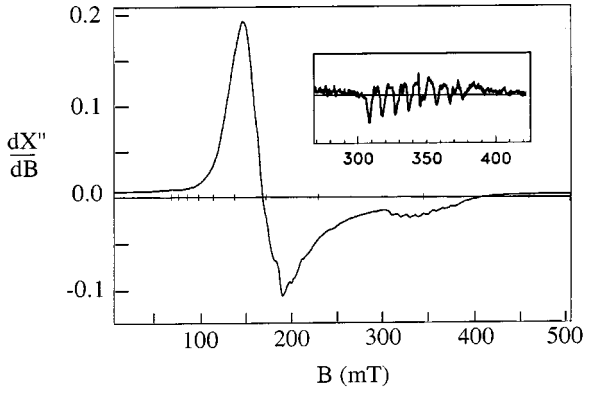

Figure 6. X-band EPR spectrum of **4** (ca. 5×10^{-4} M) in frozen DMF solution recorded at 10 K with a power of 10 mW (33 dB) at a frequency of 9.64 GHz; inset: second derivative signal (amplitude modulation)

Conclusion

Using two different amine/sulfur ligands, S_2N_2 and $S_2N_3^{py}$, we have obtained two new Co^{II} complexes. While the instability of the [$Co^{II}S_2N_3^{py}$] species prevented a complete study, the [$Co^{II}S_2N_2$]$_2$ dimer has been fully characterized both in the solid state and in solution. Its dimeric structure leads to an S_3N_2 coordination sphere for each Co centre, which is probably responsible for its increased stability; this complex can be reversibly oxidized by one and two oxidizing equivalents. A strong resonance Raman band at 220−230 cm^{-1} constitutes the vibrational signature of the Co_2S_2 core in the fully reduced as well as in the mixed valence state of the dimer.

Experimental Section

Caution: Attention is drawn to the highly toxic nature of 2-aminobenzenethiol. − All the syntheses were performed under argon using standard Schlenk techniques. All solvents were dried and distilled prior to use.

Physical Measurements: Electronic spectra were recorded with a Uvikon 820 double-beam spectrophotometer. − ^{1}H NMR spectra were recorded at 300 K with a Bruker ARX-250 spectrometer controlled by UXNMR software run with an Aspect 1 station. Chemical shifts are reported downfield from TMS. Magnetic susceptibilities of powder samples were measured in the range 2−293 K with a SQUID magnetometer (MPMS, Quantum Design) in a 1-T external magnetic field. Diamagnetic corrections were applied by using Pascal's constants. − X-band EPR spectra of samples in frozen solutions in quartz cells ($d = 0.3$ mm) were measured with a Bruker ESP 300E spectrometer operating at 9.5 GHz, equipped with an Oxford Instruments EPR 910 helium-flow cryostat. − Cyclic voltammetry and coulometric experiments were performed with Radiometer equipment using solutions containing 0.1 M tetrabutylammonium chloride (Bu_4NCl) or hexafluorophosphate (Bu_4NPF_6) as supporting electrolytes. The electrode system consisted of an NaCl-saturated calomel electrode (SCE) as the reference, a platinum auxiliary electrode, and a glassy carbon working electrode. The potential sweep rate was 50 mV s^{-1}. Ferrocene was used as an internal standard [$E_{1/2}$ (ferricinium/ferrocene) = +450 mV vs. SCE]. Spectroelectrochemistry was performed using an EG & G PAR-173 apparatus and a Varian spectrophotometer. − Electrospray mass spectra were measured from samples in dichloromethane solution. − Elemental analyses were carried out by the microanalysis service at the Paris VI University. − The crystal structure was solved by the X-ray service at the Paris VI University.

[S_2N_2Zn] {[2,3-Bis(2-mercaptoanilino)butane]zinc(II), 1}: The zinc complex **1** was prepared according to the published procedures of Bayer et al.[5] and Corbin et al.[6]

[$S_2N_2Co^{II}$]$_2$ (2): 2 equiv. of aqueous NaOH (108 μL of a 2 N solution) was added to a solution of [S_2N_2Zn] (40 mg, 0.11 mmol) in DMF (5 mL). After stirring for 10 min, the white precipitate of $Zn(OH)_2$ was removed. A solution of $CoCl_2{\cdot}6H_2O$ (26 mg, 1 equiv.) in DMF was then added dropwise to the free dithiolate ligand. Addition of aqueous NaOH (2 N, 50 μL) resulted in a purple solution of [$S_2N_2Co^{II}$]$_2$. After removal of the DMF in vacuo, the complex was redissolved in CH_2Cl_2 and precipitated by the addition of pentane. The microcrystalline purple precipitate was collected by filtration and washed with methanol (75 mg, 95% yield). Diffusion of pentane into a dichloromethane solution of **2** yielded purple crystals. − $C_{32}H_{36}Co_2N_4S_4{\cdot}0.5CH_2Cl_2$ (706.33): calcd. C 51.01, H 4.87, N 7.32; found C 50.9, H 4.2, N 7.4. − MS (ESI^+): *m*/*z* (%) = 718 (100) {[$S_2N_2Co^{II}$]$_2$ − 4 H; imine formation}. − ^1H NMR (250 MHz, [D_6]DMSO, in the presence of 1 equiv. of 1 M Bu_4NOH in MeOH; the proton resonances were assigned on the basis of their intensity ratios and ^1H longitudinal relaxation times (T_1), which have been correlated to the Co···H distances): CH_3: δ = −18 (s, 12 H), T_1 = 29 ms, Co(1)−C(23) = 3.583(18) Å; H(21): δ = +166 (s, 4 H), T_1 = 30 ms, Co(1)−C(21) = 2.855(15) Å; H(3) and/or H(6): δ = −101 (s, 4 H), T_1 = 32 ms, and δ = −107 (s, 4 H), T_1 = 61 ms, Co(1)−C(3) = 4.336(6) Å and Co(1)−C(6) = 4.167(7) Å; H(4) and/or H(5): δ = +12 (s, 4 H), T_1 = 261 ms and δ = +16.5 (s, 4 H), T_1 = 144 ms, Co(1)−C(4) = 5.263(6) Å and Co(1)−C(5) = 5.170(6) Å.

[$S_2N_3^{py}Zn$] ({2,6-Bis[1-(2-mercaptoanilino)ethyl]pyridine}zinc(II), 3): A solution of $NaBH_4$ (0.717 g, 4.5 mmol) in EtOH/DMF (1:4; 125 mL) was added dropwise to a solution of {2,6-bis[2-(2-mercaptophenyl)-1-methyl-2-azaethenyl]pyridine}zinc(II)[23] (2.0 g, 4.5 mmol) in DMF (120 mL) cooled to 0 °C. The initially red solution became progressively more orange. After stirring at room temperature for 2 h, the DMF and ethanol were removed in vacuo. The residual oil was dissolved in methanol and the product was precipitated by the addition of twice the volume of water. The resulting orange precipitate was isolated in quantitative yield (2.0 g, 100%). − $C_{21}H_{21}N_3S_2Zn$ (444.92): calcd. C 56.69, H 4.76, N 9.44; found C 56.93, H 4.84, N 9.24. − ^1H NMR (250 MHz, [D_6]DMSO): δ = 1.37 (m, 6 H, CH_3), 4.49 (d, 2 H, CH), 5.76 (m, 2 H, NH), 6.87 (m, 4 H, ArH), 7.13 (d, 2 H, ArH), 7.21 (d, 2 H, ArH), 7.68−8.12 (m, 3 H, pyrH). − MS (EI): *m*/*z* (%) = 443 (100) {[$S_2N_3^{py}Zn$] − H}, 428 (60) {[$S_2N_3^{py}Zn$] − CH_3 − H}, 318 (70) {[$S_2N_3^{py}Zn$] − C_6H_5S}.

[$S_2N_3^{py}Co^{II}$] (4): 2 equiv. of aqueous NaOH (2 N, 90 μL) was added to a solution of [$S_2N_3^{py}Zn$] (40 mg, 0.09 mmol) in DMF (5 mL). After removing $Zn(OH)_2$, a solution of $CoCl_2{\cdot}6H_2O$ (21 mg, 1 equiv.) in DMF was added dropwise to the free ligand solution to give a yellow-green solution of **4**. After partial evaporation of the DMF in vacuo, addition of anhydrous diethyl ether (40 mL) led to the deposition of a light-green precipitate, which remained stable only at 0 °C and under argon. The complex was stored at −40 °C and was handled under anaerobic conditions at low temperatures at all times. − ^1H NMR (250 MHz, [D_7]DMF, −40 °C): δ = −27.13 (s, 1 H), −25.47 (s, 1 H), −24.44 (s, 1 H), −20.19 (s, 1 H), −18.53 (s, 1 H), −14.23 (s, 1 H), −9.74 (s, 1 H), −4.31 (s, 1 H), +9.82 (s, 1 H), +11.96 (s, 3 H, CH_3), +14.09 (s, 1 H), +16.31 (s, 1 H), +18.31 (s, 3 H, CH_3), +94.06 (s, 1 H), +101.20 (s, 1 H), +108.83 (s, 1 H), +161.30 (s, 1 H).

X-ray Crystallographic Data and Structure Refinement: Crystals of $C_{32}H_{36}Co_2N_4S_4$ (**2**) suitable for X-ray analysis were obtained by vapour diffusion of pentane into a dichloromethane solution of the complex. A selected crystal of dimensions 0.2 × 0.3 × 0.4 mm was attached to the tip of a glass fibre. Accurate cell dimensions and an orientation matrix were obtained by least-squares refinement of 25 accurately centred reflections with a Nonius-CAD4 diffractometer using graphite-monochromated Mo-K_α radiation. The regular decay (ca. 28%) of two checked reflections data were scaled. Absorption corrections were applied using the DIFABS method with $T_{min.}$ = 0.86 and $T_{max.}$ = 1.[24] Collection parameters and selected crystallographic data for **2** are listed in Table 1 and 2. The data were corrected for Lorentz and polarization effects. Computations were performed using the PC version of CRYSTALS.[25] Scattering factors and corrections for anomalous dispersion were taken from Cromer.[10] The structure was solved by direct methods using SHELXS[27] and refined by full-matrix least squares with anisotropic thermal parameters for all atoms except disordered carbon atoms. The four carbon atoms of the 1,2-dimethylethyl bridge were disordered and were each located in two different sites with occupancies of 0.5, namely (C-21, C-22), (C-23, C-24), (C-31, C-32), (C-33, C-34). The complex is made up of two asymmetric units related through an inversion centre. Hence, all the unlabelled atoms are related to the labelled ones through the inversion centre symmetry operation. Atoms C-22, C-24, C-32, and C-34 are omitted for the sake of clarity. Crystallographic data (excluding structure factors) for the structure reported in this paper have been deposited with the Cambridge Crystallographic Data Centre as supplementary publication no. CCDC-151295. Copies of the data can be obtained free of charge on application to the CCDC, 12 Union Road, Cambridge CB2 1EZ, U.K. [Fax: (internat.) + 44-1223/336-033; E-mail deposit@ccdc.cam.ac.uk]

Resonance Raman Spectroscopy: The resonance Raman spectra were obtained with a J. Y. U1000 double monochromator, equipped with an AsGa photomultiplier and photon-counting electronics. Excitation wavelengths from Ar^+ and Kr^+ lasers (30−50 mW power) were used. The mechanical slit width was set at 400 μm, so that the spectral slit width varied from 2 cm^{-1} at 676.4 nm to 4 cm^{-1} at 528.7 nm. The complexes were studied in CH_2Cl_2 and DMF solutions in a rotating cell (concentration 1 mM). The 657 cm^{-1} band of DMF was used to measure the relative intensities of the bands (based on peak heights) at the various excitation wavelengths.

Supporting Information: Figures S1−S6 show the magnetic susceptibility of **2** as a function of temperature, the cyclic voltammogram of **2** in DMF, the ^1H NMR spectrum of **2**, the ^1H NMR spectrum of **4**, and the resonance Raman frequencies of **2** and **2a** (see footnote on page 1).

Acknowledgments

This work was funded by the European Commission TMR-NOHEMIP research network no. ERBFMRXCT98−0174. We wish to thank J. Vaissermann for performing the X-ray structure determination of the binuclear Co complex. D. B. gratefully acknowledges Rhône−Poulenc for a fellowship.

[1] R. H. Holm, P. Kennepohl, E. I. Solomon, *Chem. Rev.* **1996**, *96*, 2239−2314.
[2] O. Y. Gavel, S. A. Bursakov, J. J. Calvete, G. N. George, J. J. G. Moura, I. Moura, *Biochemistry* **1998**, *37*, 16225−16232.

[3] M. Kobayashi, S. Shimizu, *Eur. J. Biochem.* **1999**, *261*, 1−9.
[4] P. T. Rajagopalan, S. Grimme, D. Pei, *Biochemistry* **2000**, *39*, 779−790.
[5] E. Bayer, E. Breitmayer, *Chem. Ber.* **1968**, *101*, 1579−1593.
[6] J. L. Corbin, D. E. Work, *Can. J. Chem.* **1974**, *52*, 1054−1058.
[7] V. L. Goedken, G. G. Cristoph, *Inorg. Chem.* **1973**, *12*, 2316−2320.
[8] M. F. Corrigan, K. S. Murray, R. M. Sheahan, B. O. West, G. D. Fallon, B. M. Gatehouse, *Inorg. Nucl. Chem. Lett.* **1975**, *11*, 625−628.
[9] K. D. Karlin, D. L. Lewis, H. N. Rabinowitz, S. J. Lippard, *J. Am. Chem. Soc.* **1974**, *96*, 6519−6521.
[10] J. C. Noveron, M. M. Olmstead, P. K. Mascharak, *J. Am. Chem. Soc.* **1999**, *121*, 3553−3554.
[11] M. J. Baker-Hawkes, Z. Dori, R. Eisenberg, H. B. Gray, *J. Am. Chem. Soc.* **1968**, *90*, 4253−4259.
[12] J. H. Enemark, W. N. Lipscomb, *Inorg. Chem.* **1965**, *4*, 1729−1734.
[13] S. C. Shoner, D. Barnhart, J. A. Kovaks, *Inorg. Chem.* **1995**, *34*, 4517−4518.
[14] A. Böttcher, H. Elias, E.-G. Jager, H. Langfelderova, M. Mazur, L. Müller, H. Paulus, P. Pelikan, M. Rudolph, M. Valko, *Inorg. Chem.* **1993**, *32*, 4131−4138.
[15] U. Küsthardt, R. W. Albach, P. Kiprof, *Inorg. Chem.* **1993**, *32*, 1838−1843.
[16] C. A. Ghilardi, C. Mealli, S. Midollini, V. I. Nefedov, A. Orlandini, L. Sacconi, *Inorg. Chem.* **1980**, *19*, 2454−2462.
[17] P. K. S. Tsang, P. Cofre, D. T. Sawyer, *Inorg. Chem.* **1987**, *26*, 3604−3609.
[18] T. G. Spiro, R. S. Czernuszewicz, S. Hans, *Biological Applications of Raman Spectroscopy* (Ed.: T. G. Spiro), Wiley, New York, **1988**, vol. 3, pp. 523−554.
[19] C. R. Andrew, J. Sanders-Loehr, *Acc. Chem. Res.* **1996**, *29*, 365−372.
[20] K. Kanamori, S. Ino, Y. Mizumo, K. Kawai, J. Hidaka, *Bull. Chem. Soc. Jpn.* **1989**, *62*, 2375−2378.
[21] S. Hans, R. S. Czernuszewicz, T. G. Spiro, *J. Am. Chem. Soc.* **1989**, *111*, 3496−3504.
[22] I. Michaud-Soret, K. K. Andersson, L. Que, *Biochemistry* **1995**, *34*, 5504−5510.
[23] L. F. Lindoy, D. H. Busch, *Inorg. Chem.* **1974**, *13*, 2494−2498.
[24] N. Walker, D. Stuart, *Acta Crystallogr.* **1983**, *A39*, 158−166.
[25] D. J. Watkin, C. K. Prout, R. J. Carruthers, P. W. Betteridge, *CRYSTALS*, University of Oxford, U.K., **1996**.
[26] D. T. Cromer, *International Tables for Crystallography*, Kynoch Press, Birmingham, U.K., **1974**, vol. IV.
[27] G. M. Sheldrick, *SHELXS − Program for the Solution of Crystal Structures*, University of Göttingen, Germany, **1986**.

Received October 27, 2000
[I00410]